Title

Long-term leaf C:N ratio change under elevated CO2 and nitrogen deposition in China: Evidence from observations and process-based modeling

Authors

Sheng, Mingyang
Tang, Jinyun
Yang, Dawen
et al.

Publication Date

2021-12-01

DOI

10.1016/j.scitotenv.2021.149591

Long-term leaf C:N ratio change under elevated CO_2 and nitrogen deposition in China: evidence from observations and process-based modeling

Mingyang Sheng[1], Jinyun Tang[2], Dawen Yang[1*], Joshua Fisher[3], Han Wang[1], and Jens Kattge[4]

[1]State Key Laboratory of Hydroscience and Engineering, Department of Hydraulic Engineering, Tsinghua University, Beijing, China

[2]Climate and Ecosystem Sciences Division, Climate Sciences Department, Lawrence Berkeley National Laboratory, Berkeley, California, USA

[3]Jet Propulsion Laboratory, California Institute of Technology, Pasadena, California, USA

[4]Max-Planck-Institute for Biogeochemistry, 07745 Jena, Germany

*Corresponding author: Dawen Yang yangdw@tsinghua.edu.cn

Highlights:

- Leaf C:N ratio decreased in southern China, but increased in western and northern China in the past 5 decades.
- N deposition was a dominant factor driving C:N ratio change in most areas, while elevated CO_2 dominated in low N deposition area.
- Leaf C:N ratio shifts were more strongly constrained by N availability than by climate.

Keywords: leaf C:N ratio, data-driven modelling, process-based modelling, nitrogen deposition

Abstract

Climate change, elevating atmosphere CO_2 (eCO_2) and increased nitrogen deposition (iNDEP) are altering the biogeochemical interactions between plants, microbes and soils, which further modify plant leaf carbon-nitrogen (C:N) stoichiometry and their carbon assimilation capability. Many field experiments have observed large sensitivity of leaf C:N ratio to eCO_2 and iNDEP. However, the large-scale pattern of this sensitivity is still unclear, because eCO_2 and iNDEP drive leaf C:N ratio toward opposite directions, which are further compounded by the complex processes of nitrogen acquisition and plant-and-microbial nitrogen competition. Here, we attempt to map the leaf C:N ratio spatial variation in the past 5 decades in China with a combination of data-driven model and process-based modeling. These two approaches showed consistent results. Over different regions, we found that leaf C:N ratio had significant but uneven changes between 2 time periods (1960-1989 and 1990-2015): a 5% ± 8% increase for temperate grasslands in northern China, a 3% ± 6% increase for boreal grasslands in western China, and by contrast, a 7% ± 6% decrease for temperate forests in southern China, and a 3% ± 5% decrease for boreal forests in northeastern China. Additionally, the structural equation models indicated that the leaf C:N change was sensitive to ΔNDEP, ΔCO_2 and ΔMAT rather than ΔMAP and ecosystem types. Process-based modeling suggested that iNDEP was the main source of soil mineral nitrogen change, dominating leaf C:N ratio change in most areas in China, while eCO_2 led to leaf C:N ratio increase in low iNDEP area. This study also indicates that the long-term leaf C:N ratio acclimation was dominated by climate constraint, especially temperature, but was constrained by soil N availability over decade scale.

1 Introduction

Leaf stoichiometry examines the relationships between organism structure and function (Sardans et al., 2012; Sterner and Elser, 2002). Leaf C:N ratio can be associated with important ecological processes such as litter decomposition (d'Annunzio et al., 2008), the ability to adapt to environmental stresses (Hessen et al., 2004; Woods et al., 2003), and enzymes activities of the plant photosynthesis (Evans, 1989; Evans and Poorter, 2001). Lower leaf nitrogen status (higher C:N ratio) increases non-stomatal limitations on photosynthesis through the impairment of carboxylation capacity, photochemical efficiency, and osmotic protection (Wright et al., 2005). In contrast, higher foliar N concentration (lower C:N ratio) may be associated with larger C-assimilation and growth-rate capacities (Sterner and Elser, 2002). Given the tight connection between leaf C:N ratio and productivity at the canopy scale (Reich, 2012), leaf C:N ratio is an important parameter in terrestrial ecosystem model and plays a vital role in carbon sequestration projection (Caldararu et al., 2020; Ghimire et al., 2016; Meyerholt and Zaehle, 2015).

Leaf C:N ratios are driven by variation in plant physiology, soil biogeochemistry, and plant community composition (Reich and Oleksyn, 2004). In the past 50 years, climate change (CLIM), elevating atmosphere CO_2 (eCO_2) and increased nitrogen deposition (iNDEP) were likely to have changed the biogeochemical interactions between plants, microbes and soil, which further modified plant leaf C:N ratio and their carbon assimilation capability. There are mainly two hypothesizes predicting ecosystem level leaf C:N ratio acclimation under environment change: (a) the climate envelope theory, and (b) the theory of trade-off between resources acquisition and conservation. The climate envelope theory assumes that local environment constrains the species trait range, thus environmental change is likely to filter out inappropriate species or trait range, resulting in plant trait being environment selected (Atkin et al., 2015;

Hijmans and Graham, 2006; Kattge and Knorr, 2007; Wright et al., 2005). For example, low leaf C:N ratio means an adaptation that enhances metabolic activity and growth rates under the low temperatures. Within species, populations from colder habitats often have greater leaf N (lower C:N ratio) (Reich and Oleksyn, 2004; Weih and Karlsson, 2001; Woods et al., 2003). So, it is likely that the ecosystem level leaf C:N ratio would increase under climate warming, and there would be similar sensitivities of leaf C:N ratio change in both spatial and temporal variation to environment factors.

On the other hand, the theory of trade-off between resources acquisition and conservation assumes that plants will adjust relevant traits to optimize the balance between resources uptake and the cost of acquisition (Kong et al., 2014; Reich, 2014). Leaf N concentration typically reflect soil N availability (Vitousek et al., 1995), and more soil N means less cost of acquisition for plants to hold more N. This hypothesis is partly supported by short-term experiments. Warming experiments could increase leaf N concentration, which is linked to increases in N mineralization, cycling rates and availability due to enhanced soil microbial activity (Bai et al., 2013). In CO_2 enrichment experiments, decreasing leaf N concentration and therefore lower photosynthesis capacity were observed, especially in nitrogen limited environment (Ainsworth and Long, 2005; Crous et al., 2010; Ellsworth et al., 2004). By contrast, nitrogen fertilization is likely to restore leaf N concentration and to stimulate photosynthesis (Liu et al., 2011; McCarthy et al., 2006; Norby et al., 2003; Palmroth et al., 2006; Sigurdsson et al., 2013). Additionally, several global meta-analysis studies found that leaf C:N ratio shows a strong positive correlation to eCO_2 and a negative correlation to nitrogen addition for nearly any species in any locations in the world (Du et al., 2019; Huang et al., 2015; Li et al., 2013; Yang et al., 2011; Yue et al., 2017). Hence, climate warming tends to increase leaf N concentration (decrease leaf C:N ratio)

98 by accelerating the decomposition and mineralization of soil organic matter, which increases the
99 availability of soil N. Meanwhile, eCO_2 could enhance plant C acquisition but increase the
100 burden of N uptake, leading a higher leaf C:N ratio. Human induced N addition (iNDEP) could
101 also decrease the leaf C:N ratio by increasing soil N availability. Therefore, the trade-off theory
102 implies the possibility that environment factors sensitivities of leaf C:N ratio change in spatial
103 and temporal scales could be different.

104 Despite its significance in understanding ecosystem dynamics, the large-scale pattern of
105 long-term leaf C:N stoichiometry change under environment changes and its sensitivity to
106 diverse environmental factors under natural conditions are still unclear. This uncertainty emerges
107 from several reasons. First, as mentioned above, the mechanisms and processes related to leaf
108 C:N ratio variation are complicated. Different hypotheses lead to opposite results. Second, the
109 combined effects of environmental factors are difficult to predict. For instance, the opposite
110 impacts of eCO_2 and iNDEP may offset the final direction of change in leaf C:N stoichiometry,
111 making the compound response to combined influences of climate, eCO_2 and iNDEP weak and
112 unclear (Yue et al., 2017). Third, synthesis are often based on small spatial scale short-term
113 experiments, which seem to overestimate the response of long-term plant acclimation at larger
114 spatial scales (Leuzinger et al., 2011).

115 Among the limited number of in-situ field studies, their observations were inconsistent.
116 Natural plants in China experienced nearly 30% increasing of leaf N concentration between
117 1980s and 2010s (Liu et al., 2013). By contrast, in Russia and Western Europe, leaf N
118 concentration had an 8% decrease (Jonard et al., 2015; Soudzilovskaia et al., 2013), and in
119 America about 20% decrease in the similar time period (McLauchlan et al., 2010). Nonetheless,
120 in recent years, thanks to efforts of the whole plant science community, more plant stoichiometry

121 trait data become available, which include the TRY database (https://www.try-
122 db.org/TryWeb/Home.php) (Kattge et al., 2011). This in conjunction with non-linear regression
123 tools development for large-scale plant trait mapping (Butler et al., 2017; Moreno-Martinez et
124 al., 2018) makes it possible to use data-driven methods to establish a large-scale map of leaf
125 stoichiometry change, which would help us to understand the inconsistency in different plot scale
126 studies under complex environment conditions, to discover the dominant environment factor of
127 leaf C:N stoichiometry, and to test theories and hypotheses related to leaf C:N stoichiometry
128 change. On the other hand, given the observed large sensitivity of leaf C:N ratio to environment
129 change, more and more land surface models (LSM) are replacing the fixed stoichiometry plant
130 formulation with a flexible CN ratio capability to improve the estimates of gross primary
131 productivity (GPP) or net primary productivity (NPP) (Caldararu et al., 2020; Ghimire et al.,
132 2016; Meyerholt and Zaehle, 2015). This advance in process-based modeling provides another
133 tool to predict long-term leaf C:N ratio change at the large spatial scale under environment
134 changes. Moreover, the sensitivity experiments by numerical model can also be used to test
135 hypotheses related to leaf C:N ratio change.

136 In this study, we employ both data-driven modeling and process-based modeling to map the
137 large-scale leaf C:N ratio change and analyze their sensitivities to environmental factors. We
138 selected China as the study region, given its NDEP experienced the largest increase in the world
139 in the past thirty years (Liu et al., 2013) and uneven distribution in different regions, e.g., a 0.5
140 gN m^{-2} yr^{-1} NDEP in Tibetan Plateau vs 5 gN m^{-2} yr^{-1} NDEP in eastern China (Fig S1).
141 Moreover, the leaf trait data in China have covered a good spatial and temporal distribution (Fig
142 S2).

143 Our study was guided by the following questions:

1) What is the spatiotemporal pattern of leaf C:N ratio change in the past 50 years in China? Does it have large differences in different regions or for different plant functional types (PFT)?

2) What was the most sensitive environment factor for leaf C:N ratio change in China, climate change, eCO_2 or iNDEP? Were leaf C:N ratio change determined by climate envelope or determined by the balance between soil nitrogen supply and plant demand?

3) Does process-based modelling agree with data-driven modeling in inferred leaf C:N pattern and changes? And how well does the hypothesis in the process-based model work? What is its implication to carbon cycling modelling?

2 Material and Methods

In this study, we focus on the spatiotemporal variation of the ecosystem level leaf C:N ratio in China. We firstly collected in-situ plant traits data, and then used two methods to derive a spatiotemporal conterminous leaf C:N ratio map: (1) random forest based up-scaling of in-situ trait measurements, and (2) large scale process-based modeling using the Community Land Model version 5.0 (Lawrence et al., 2019).

2.1 In-situ plant traits data collection and data gap-filling

The in-situ plant trait database in this study include two variables: leaf carbon concentration (LCC in mgC g^{-1}) and leaf nitrogen concentration (LNC in mgN g^{-1}). These traits data consist of two parts: one is obtained from the TRY database, and the other is collected from the literature using *ISI Web of Knowledge*, *Google scholar* and *CNKI* website. Overall, we collected 28406 records worldwide, where 24529 records were contributed from the TRY database (2978 plots in China), and the other 3931 records (all in China) were collected from the

literature. The detail of literature sources and plot location distribution are in Table S1 and Figure S2, respectively.

To improve the data consistency through pre-processing, we eliminated unreasonable data and then gap-filled using the method from Moreno-Martinez et al., (2018) (see Appendix 1). Moreover, to explore the leaf trait temporal variation, we made two vital assumptions: 1) if there is not any temporal information in the original datasets, the measurement time of the plot was assigned as 2 years before publication time, following the method in Liu et al., (2013); and 2) the LNC and LCC trait measurement, mainly sampling fully expanded and hardened leaves (presumably photosynthetically more productive) from adult plants (Cornelissen et al., 2003), were representative of the decadal homeostatic status. The second assumption also helps to reduce the bias resulting from uncertainty in determining the sampling time.

In the gap filling process, we used the python based random forest implementation sklearn.ensemble.RandomForestRegressor (https://scikit-learn.org/stable/modules/generated/sklearn.ensemble.RandomForestRegressor.html?highlight=random%20forest#sklearn.ensemble.RandomForestRegressor) (Pedregosa et al., 2011) and segmented the predictors into 4 categories: taxonomic hierarchies, plant structure, multiple annual mean environment factors (representing long-term steady climate), and their decadal variance (representing temporal climate change) (See Table S2).

For climate input data, we chose the monthly 0.5x0.5 degree CRU TS 4.02 global climate dataset for the period of 1950-2015 (https://crudata.uea.ac.uk/cru/data/hrg/) (Harris et al., 2014). The monthly cloudiness, frost day, potential evaporation, precipitation, diurnal temperature range, mean air temperature were acquired from the datasets. A yearly 0.9x1.25 degree global nitrogen deposition (NDEP) dataset produced by atmospheric chemical transport model was

189 acquired from University Corporation for Atmospheric Research (NCAR) for the period of 1960-
190 2015, regrided to 0.25x0.25 degree, and then corrected using site observation from Lü and Tian
191 (2007). The NDEP spatiotemporal pattern in China from the corrected dataset is consistent with
192 other observation studies (See Fig. S1, Zhu et al. (2015) and Yu et al. (2019)). The global spatial
193 average CO_2 concentration time serial was acquired from NCAR for the period of 1960-2015.
194 R^2 score was used to evaluate the performance of the gap-filling processes. Fig. S3
195 showed the performance in gap-filling with a high R^2 both in training process (0.68 for LNC and
196 LCC) and in validation process (0.62 for LNC and 0.64 for LCC).

197 2.2 Random forest up-scaling of in-situ measurements of plant traits

198 After data pre-processing, we up-scaled the in-situ measurement to the 0.25-degree grid
199 according to the major PFT information for a given grid, and then interpolated the results to
200 other grids using the random forest algorithm, following Moreno-Martinez et al., (2018) (see
201 Appendix S2 for detail). In this process, an accurate high spatial resolution land cover data is
202 essential, and for this we used the Land Use Harmonization 2 (LUH2, luh.umd.edu/data.shtml)
203 PFT datasets, because it used a robust classification method, covering over 15 PFTs at a spatial
204 resolution of 0.25 degree with sub-grid PFT information worldwide (Lawrence et al., 2016).
205 Here, we assumed that there was no land use/cover change (LUCC) or plant functional type
206 change in China in the past 5 decades. This assumption is partly supported by the LUCC studies
207 for the past 3 decades (the expansion of cultivated land was less than 40 thousand km^2 and the
208 degradation of forest was less than 20 thousand km^2 in the past 30 years in China, which are tiny
209 numbers compared to the total rural area 8533 thousand km^2 in China (Liu et al., 2010; Song and
210 Deng, 2017), see Table S3).

The representativeness of climate and NDEP condition of global plot samples with respect to the China region was also tested in this study. The mean annual precipitation (MAP), mean annual air temperature (MAT), and PFT of plot samples and China region are presented in Fig. S4. The climate of plot samples has a similar distribution with the China region across different PFTs. For example, the MAT of boreal grassland ranges from -10.4 ℃ to 8.5℃ for plot samples vs from -7.9 ℃ to 11.1℃ for the China region. The MAP of grassland ranges from 250 mm to 1550 mm for plot samples vs from 305mm to 1241 mm for the China region (See Table S5). The NDEP probability density curves across different PFTs are presented in Fig S5. The probability density curves of the plot samples are also representative of the typical distributions of China regions.

Fig. S6 showed the performance in up-scaling, with R^2 0.64 for LNC and 0.72 LCC in the training process, and 0.35 for LNC and 0.46 for LCC in validation process, respectively. The R^2 for up-scaling is also comparable to other studies with a range from 0.25 to 0.56 (Table S4). Next, given the relatively low spatial resolution of the CRU dataset (0.5 degree) applied to China at and to ensure the consistency with land surface model meteorology forcing, we employed the validated model (regression relationships) with a new climate dataset of a finer spatial resolution (0.25 degree) to predict a relatively finer up-scaled map for LNC and LCC (See 2.3 for the detail of the dataset).

2.3 Process-based modelling: Community Land Model version 5.0

A state-of-the-art process-based model, Community Land Model version 5.0 (CLM5.0), was selected as an alternative method to analyze the leaf C:N ratio change in China. CLM5.0 is selected because 1) as a newly released simulation tool, CLM5.0 has the capability of simulating leaf carbon mass, leaf nitrogen mass, and leaf C:N ratio change with a process-based scheme of

234 flexible leaf stoichiometry; 2) CLM5.0 couples plant C, N and leaf stoichiometry explicitly, thus
235 enabling us to analyze the impact of leaf stoichiometry on plant carbon and nitrogen cycle
236 modelling.

237 CLM5.0 is the default land component model for the Community Earth System Model
238 version 2 (CESM2) (http://www.cesm.ucar.edu/models/cesm2/). As a land surface model,
239 CLM5.0 represents processes such as soil and plant hydrology, river routing, coupled carbon and
240 nitrogen cycling, and crop dynamics. We refer more detail of the CLM5.0 to its full technical
241 description (http://www.cesm.ucar.edu/models/cesm2/land/CLM50_Tech_Note.pdf) (Lawrence
242 et al., 2019) and below only give a brief introduction to leaf stoichiometry or flexible CN ratio
243 parameterization in the model. CLM5.0 assumes that plant take up nitrogen at the cost of energy
244 in the form of carbon (Doughty et al., 2018), which thence allows plant to adjust their CN ratio
245 by making trade-off between nitrogen uptake and associated carbon expenditure (Ghimire et al.,
246 2016). This flexible CN ratio also results in a new nitrogen limitation scheme differing from
247 CLM4.5 by removing the instantaneous down-regulation of potential GPP induced by
248 insufficient soil mineral nitrogen to support plant demand. More details are described in
249 Appendix S3.

250 We conducted CLM5.0 simulations of China at 0.25° x 0.25° and half-hourly
251 spatiotemporal resolution for the period from 1960 to 2015. In order to reduce the bias in climate
252 forcing, we combined data from two sources, 1) daily surface air temperature (mean, maximum
253 and minimum air temperature), relative humidity, wind speed and sunshine duration from 736
254 stations across China from 1960 to 2015 procured from China Meteorological Administrations
255 (http://cdc.nmic.cn). 2) China Gridded Daily Precipitation Product with a 25 km spatial
256 resolution across China from 1960 to 2015 obtained from China Meteorological Administrations

(http://cdc.cma.gov.cn/dataSetLogger.do?changeFlag=dataLogger). These two datasets are then used to derive a forcing data at 0.25° x 0.25° degree and 3-hourly spatiotemporal resolution in China for the period from 1960 to 2015, following the method in Lei et al. (2014). We also replaced the default soil texture data with a local version at 1 km spatial resolution (Shangguan et al., 2012). Other input datasets, including land cover, nitrogen deposition, aerosol deposition, CO_2 concentration, adopted the default configuration for CLM5.0 (Lawrence et al., 2019). For a consistent comparison, it is noted that we used the same climate, land cover, nitrogen deposition and CO_2 concentration datasets in the data-driven approach.

In order to separate the impact from different environmental factors, we devised simulations of four scenarios.

- S0: static climate with all environmental factors being constant,
- S1: climate change with other factors being constant,
- S2: climate change and elevated atmosphere CO_2 concentration, and
- S3: climate change, elevated atmosphere CO_2 concentration and nitrogen deposition change.

Based on these four simulations, the influence of climate change ('CLIM') was estimated from the difference between S1 and S0. The effect of CO_2 enrichment ('eCO_2') was deducted by the difference between S2 and S1. And the impact of nitrogen deposition ('iNDEP') was estimated by the difference between S3 and S2. More details for the four-scenario model configurations are in Table S3.

Besides S0-S3, we launched another scenario simulation to test the sensitivity of carbon and nitrogen cycle to leaf C:N ratio change (by the difference of S3 and S4):

- S4: model scheme with constant leaf C:N ratio, and forced by climate change, elevated atmosphere CO_2 concentration and nitrogen deposition change.

For scenario S3 was designed to simulate the real-world condition, an evaluation of simulated nitrogen and carbon cycling was conducted by comparing S3 and observation data.

As for nitrogen cycle validation, the net soil mineralization (16 sites), plant nitrogen uptake (24 sites) and NO_x emission (27 sites) fluxes data were collected for site scale validation. Natural biological nitrogen fixation (NBNF), nitrogen deposition and denitrification fluxes at nation scale were compared to other studies to validate the gross volume of the fluxes. Overall, CLM5.0 gives a reasonable nitrogen cycle modelling, with an appropriate R^2 (>0.44) in site level validation (see Fig. S7) and consistent gross volume with other studies (see Table. S7).

For carbon cycle validation, GPP and terrestrial ecosystem respiration (TER) data in 35 flux sites were collected for site scale validation, and remote sensing based MODIS C6 GPP product (Running S., 2015) and GIMMS3g LAI product (Zhu et al., 2013) were selected for spatial pattern validation. R^2 score was selected to evaluate the performance. Overall, CLM5.0 gives a reasonable carbon cycle modelling, with a high R^2 (>0.65) in site level validation (see Fig. S8) and a high R^2 (>0.70) in spatial pattern validation (See Fig S9 and Fig S10). These performance of R^2 are also comparable to other carbon cycle modeling studies (See Table S8).

2.4 Analysis

As LCC, LNC and leaf C:N ratio are numerical ratios with significant differences between PFTs, we conducted the spatial pattern analysis by averaging over grids and PFTs rather than by over a region or whole nation. In addition, to make the modeling results more easily and simpler to understand, we rearranged the 15 PFTs classified in LUH2 into 5 PFTs, for example, by combining the 3 boreal forest PFTs (boreal evergreen needleleaf forest, boreal deciduous

needleleaf forest and boreal deciduous forest) into 1 PFT (boreal forest) (Fig. S11). In addition, due to the lack of leaf trait data for crops, and the complexity of land management in crop area, such as fertilization and seed technology improvement, we excluded crop land from this study. Moreover, given the data-driven model can only consider one PFT for one grid, we only analyzed the grids with major land cover proportion over 80%.

For temporal analysis, we separated the whole time period from 1960 to 2015 into 2 parts: 1960-1990 and 1991-2015. We defined the relative change of the variable (ΔV) as the difference between the average values in these two periods (Eq 1). This time period segmentation was determined based on 2 reasons: 1) significant environment change occurred roughly after 1990 in China, e.g., nitrogen deposition (Liu et al., 2013) and air temperature warming (Piao et al., 2010); 2), comparing a relatively long time period can ameliorate the uncertainty due to insufficient leaf data samples in the early period, especially in the 1970s and 1980s.

$$\Delta V = \frac{\overline{V_{1990-2015}} - \overline{V_{1960-1989}}}{\overline{V_{1960-1989}}} \quad \text{(Eq. 1)}$$

For statistical analysis, we used one-way ANOVA and Tukey's test to analyze the influences of different PFTs. In order to examine the effects of different factors, such as PFT, MAT, MAP, NDEP and CO_2 concentration, we used piecewise structural equation modelling for generalized linear regression models (Lefcheck and Freckleton, 2015), which was widely used in plant stoichiometry studies (Hu et al., 2021; Luo et al., 2021). In order to make the regression, boreal or temperate ecosystem was classified to 0 or 1, and grassland or forest ecosystem was classified to 0 or 1. The initial model was constructed based on the hypothesized relationships suggested in previous studies (Hu et al., 2021; Luo et al., 2021; Yuan and Chen, 2009). We fitted the component models of the piecewise structural equation model as generalized linear

regression models. Goodness-of-fit for the overall model was evaluated using Fisher's C statistic, and $p > 0.05$ showed a good fit. The standardized regression coefficient (β) for each path was then estimated, and the significance was tested.

The whole process of piecewise structural equation modelling was performed using the R package "piecewiseSEM" (Lefcheck and Freckleton, 2015). All data analyses were performed using R v.4.0.1.

3 Result

3.1 Spatial variation of multi-annual mean leaf C:N ratio

For spatial variation, leaf C:N ratio in southern China was larger than that in northern China in general (Fig 1a, 1b, and 1c). Leaf C:N ratio differed among different PFTs ($p < 0.05$; Fig 1d). Temperate ecosystem had a higher leaf C:N ratio than boreal ecosystem, and forest ecosystem had a higher leaf C:N ratio than grassland ecosystem in China by nearly all 3 approaches (temperate forest in southern China > temperate grassland in northwestern China > boreal forest in northeastern China > boreal grassland in the Tibetan Plateau). Among the three approaches, leaf C:N by plot sample data had the largest variation values with temperate forest (29.6 ± 5.6 gC gN^{-1}) , temperate grassland (25.5 ± 7.4 gC gN^{-1}), boreal forest (22.8 ± 4.7 gC gN^{-1}) and boreal grassland (20.6 ± 5.2 gC gN^{-1}), which was consistent to the results by CLM5.0 with temperate forest (28.9 ± 3.2 gC gN^{-1}) , temperate grassland (23.8 ± 3.7 gC gN^{-1}), boreal forest (23.3 ± 6.5 gC gN^{-1}) and boreal grassland (20.8 ± 5.7 gC gN^{-1}). The variation obtained by random forest approach was also consistent with other two approaches but with a smaller value with temperate forest (24.6 ± 1.2 gC gN^{-1}) , temperate grassland (22.3 ± 1.2 gC gN^{-1}), boreal forest (22.1 ± 2.0 gC gN^{-1}) and boreal grassland (20.8 ± 0.8 gC gN^{-1}).

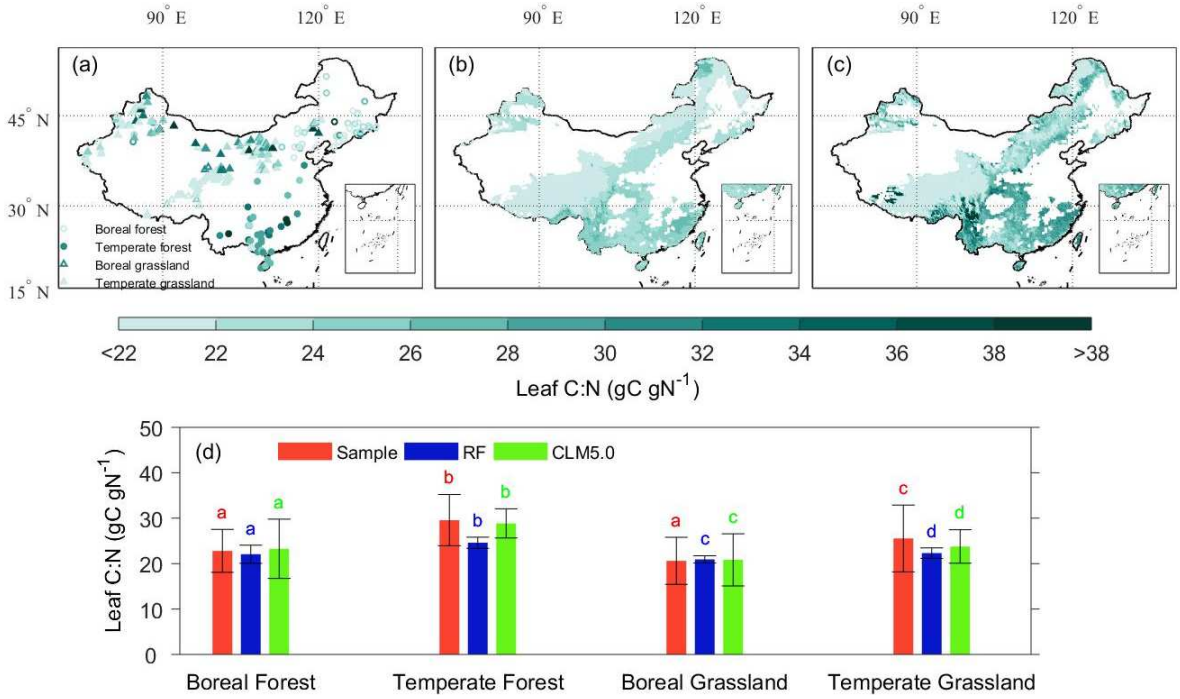

Figure 1. Spatial variation of multi-annual mean leaf C:N ratio in China (1960-2015); (a) result by plot samples, (b) result by random forest (RF) model, (c) result by CLM5.0; (d) results from all above 3 approaches averaged by PFT. Different lowercase letters in the same color on error bars indicate significant differences across different PFTs at $p < 0.05$.

3.2 Temporal variation of multi-annual mean leaf C:N ratio

For temporal variation of leaf C:N ratio change in the past 5 decades, grassland in the northwest experienced an increase in leaf C:N ratio, while forest in the southwest had a decrease (Fig 2a, 2b, and 2c). The plot samples presented a significant difference of leaf C:N ratio change between forest in the east (-9.3% ± 15.4%) and grassland in the west (+15.4% ±13.7%) ($p<0.05$, Fig 2a and 2d). The data-driven model result was consistent with respect to observed spatial distribution both in direction and magnitude with leaf C:N ratio decreasing for forest (-7.7% ± 4.2%) and increasing for grassland (+5.4% ± 6.2%) (Fig 2b and 2d). Comparatively, CLM5.0 roughly captured the direction of leaf C:N ratio change in most areas in China. However, the

magnitude of change was 50% lower in CLM5.0 than in the data-driven method (Fig 2c and 2d). If result from the data-driven model is regarded as observational benchmark, then CLM5.0 prediction with flexible CN is generally reasonable but needs to improve the leaf C:N sensitivity to environment change. In spite of their methodological differences, these two modeling approaches both showed an increasing leaf C:N ratio for temperate grassland in northern China (about +5.3% ± 8.2%) and for boreal grassland in western China (about +3.3% ± 6.6%), while a decrease for temperate forest in southern China (about -7.7% ± 6.6%) and boreal forest in northeastern China (about -3.3% ± 5.5%) (Fig 2d).

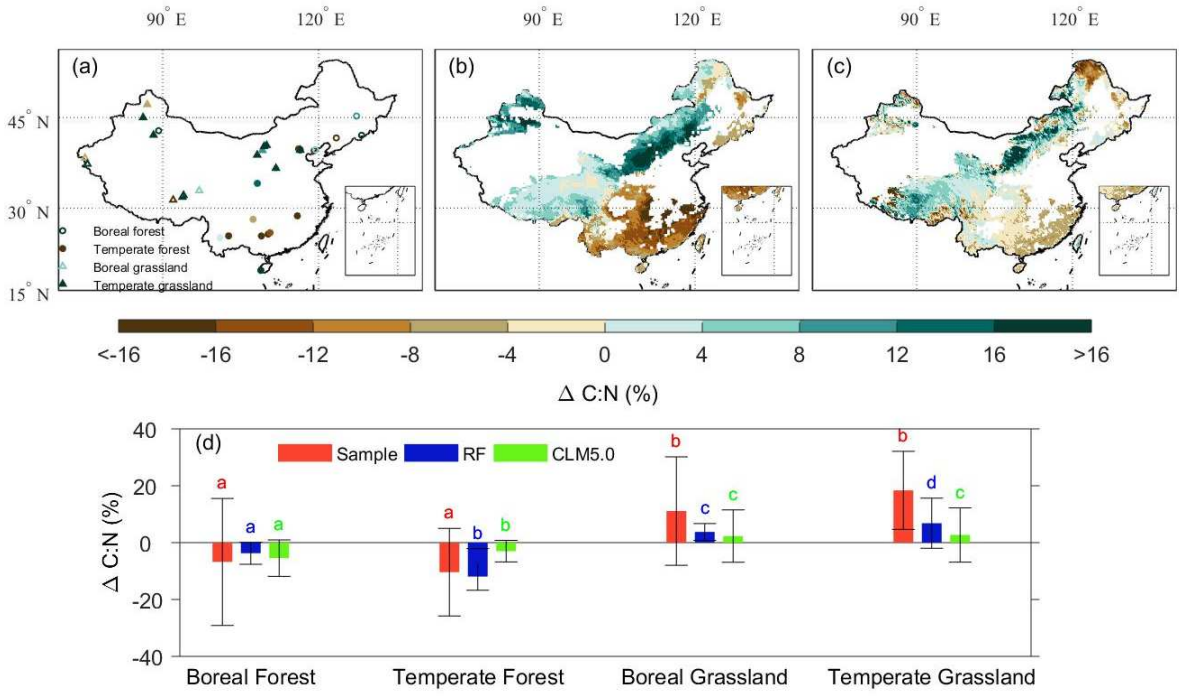

Figure 2. Temporal variation of multi-annual mean leaf C:N ratio in China; (a) result by plot samples, (b) result by random forest (RF) model, (c) result by CLM5.0; (d) results from all above 3 approaches averaged by PFT. Different lowercase letters in the same color on error bars indicate significant differences across different PFTs at $p < 0.05$.

3.3 Leaf C:N ratio spatial sensitivities to environmental factors

According to simple linear regression models, MAT and MAP were significantly positively correlated to leaf C:N ratio spatial variation from all 3 approaches ($p < 0.05$, Fig S12). The different PFTs were also significant correlated to leaf C:N ratio spatial variation ($p < 0.05$, Fig 1). Besides, MAT and MAP dominated the PFTs spatial distribution (Fig S4). The structural equation models were used to diagnose the causal relationships between these factors (Fig 3). For direct effects, climate factors and PFT had comparable importance to leaf C:N variation (β and significance were similar). Furthermore, temperature related factors (MAT and boreal or temperate ecosystem) had stronger impact on leaf C:N variation than precipitation related factors (MAP and forest or grassland ecosystem). For indirect effects, MAT rather than MAP dominated the ecosystem types (boreal or temperate), and had a further impact on leaf C:N variation. The β and significance of the paths from all three approaches were consistent with each other, and the results indicate that MAT was the most important factor to the spatial variation of multi-annual mean leaf C:N ratio.

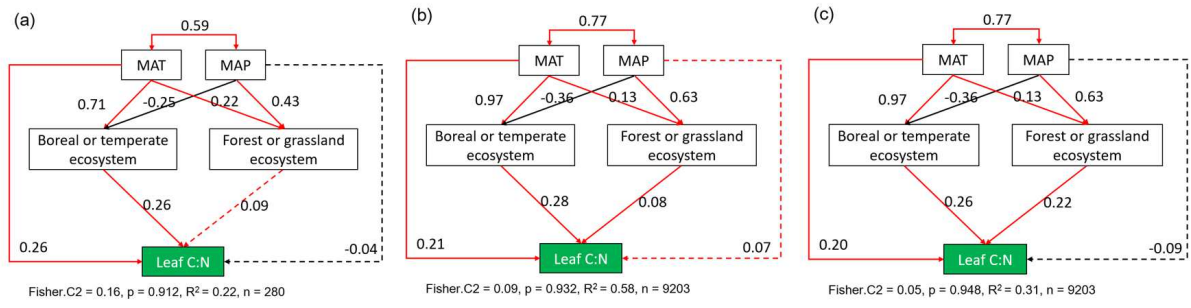

Figure 3. Structural equation models of PFT and climate as predictors of multi-annual mean leaf C:N ratio spatial variation in China. Red lines = positive and significant; black lines = negative and significant; dashed lines = insignificant. Standardized regression coefficients for each path

393 are given, and results for goodness-of-fit tests are also reported underneath each plot ($p > 0.05$
394 indicates a good fit); (a) by plot sample data, (b) by random forest model, (c) by CLM5.0

395 3.4 Leaf C:N ratio temporal sensitivities to environmental factors

396 According to simple linear regression models, ΔNDEP was significantly negatively
397 correlated to leaf C:N ratio temporal variation ($p < 0.05$), and eCO_2 was related to an increase in
398 mean leaf C:N ratio from all 3 approaches (Fig S13). The leaf C:N temporal variation of plot
399 sample data had no significant correlation with climate factors, by contrast a significantly
400 negative correlation with ΔMAP and a significantly positive correlation with ΔMAT were
401 observed from random forest model and CLM5.0. Structural equation models were used to
402 eliminate the collinearity of the factors (Fig 4). For direct effects, ΔNDEP had the strongest
403 effect to reduce Δleaf C:N (β range from -0.34 to -0.83, $p < 0.05$), by contrast ΔCO_2 played an
404 important role to increase Δleaf C:N (β range from 0.16 to 0.30, $p < 0.05$). ΔMAT also led to an
405 increase in Δleaf C:N (β range from 0.18 to 0.32, $p < 0.05$), but ΔMAP had a weaker correlation
406 to Δleaf C:N (β range from -0.05 to -0.12, $p < 0.05$). Furthermore, ecosystem types had no
407 significant relationship with Δleaf C:N, although different PFTs presented significant difference
408 in Δleaf C:N in Fig 2. This contradiction could be explained by the colinearity of ΔNDEP and
409 PFTs' distribution (r^2 range from 0.48 to 0.62, $p < 0.05$), so that ΔNDEP rather than ecosystem
410 types was likely the driving factor to Δleaf C:N. For indirect effects, ΔCO_2 significantly
411 correlated to ΔMAT ($\beta = 0.96$, $p < 0.05$) and ΔMAP (β range from 0.39 to 0.40, $p < 0.05$), and
412 had a further impact on Δleaf C:N. The β values and significance of the paths from random forest
413 model and CLM5.0 were consistent with each other, by contrast the Δleaf C:N relationships with
414 ΔCO_2 and climate were not significant by plot samples, probably due to the tiny sample size (n

415 =72). Generally, the results indicate the importance of ΔNDEP, ΔCO_2 and ΔMAT in leaf C:N
416 ratio temporal variation.

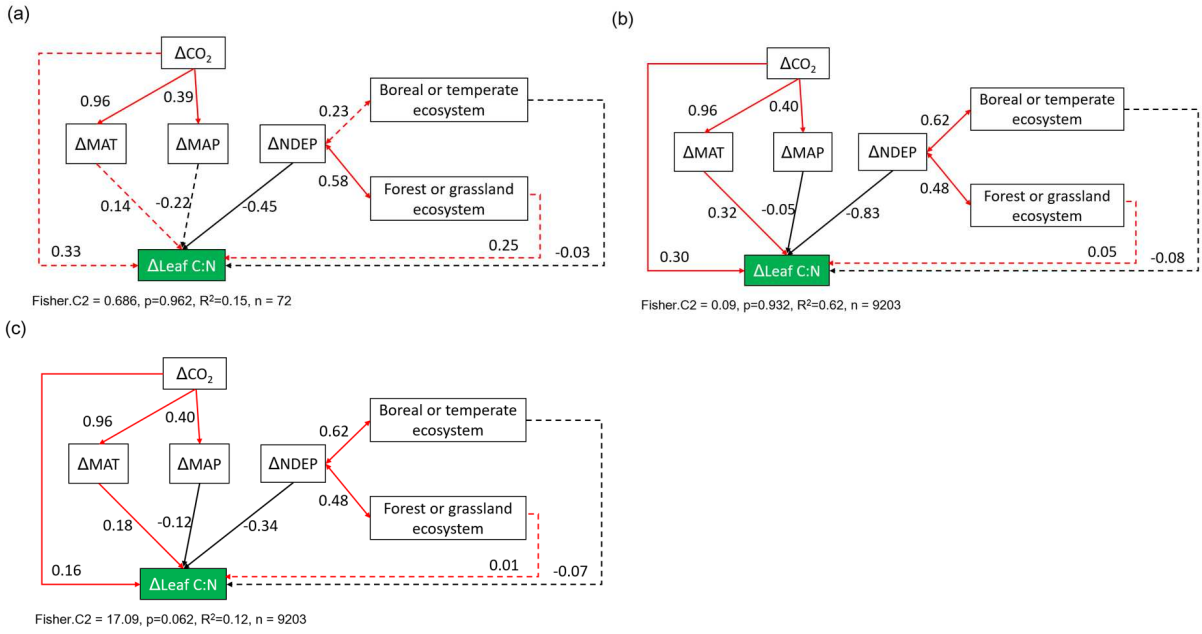

417

418 **Figure 4.** Structural equation models of PFT, climate, nitrogen deposition (NDEP) and CO_2
419 concentration as predictors of multi-annual mean leaf C:N ratio temporal variation in China. Red
420 lines = positive and significant; black lines = negative and significant; dashed lines =
421 insignificant. Standardized regression coefficients for each path are given, and results for
422 goodness-of-fit tests are also reported underneath each plot ($p > 0.05$ indicates a good fit); (a) by
423 plot sample data, (b) by random forest model, (c) by CLM5.0.

424 **4. Discussion**

425 4.1 Difference in leaf C:N spatial and temporal variation sensitivities to environmental factors

426 In our study, we find that the spatial variation of multi-annual mean leaf C:N ratio has a
427 strong correlation with long-term mean climate (especially MAT) and ecosystem types by plot
428 sample data, random forest model and CLM5.0 (Fig 1 and Fig3). The spatial variation of leaf

C:N follows the climate envelop theory. The ecosystem in a colder environment tends to have a lower leaf C:N ratio, and MAT is likely to be a driving factor to influence ecosystem types and finally leaf C:N ratio. These results were consistent with the findings at global scale (Hu et al., 2021; Reich and Oleksyn, 2004) and regional scale (Han et al., 2005; Luo et al., 2021; Tang et al., 2018).

However, the temporal variation sensitivities to environment factors are not consistent with the spatial variation sensitivities. We find that temporal Δleaf C:N was more sensitive to ΔNDEP, ΔCO_2 and ΔMAT than to ΔMAP and ecosystem types with larger β and more significant path (Fig 4). This inference was also supported by scenario simulations using CLM5.0 (Fig 5). From CLM5.0, we inferred that the decreasing leaf C:N ratio in southern China was dominated by iNDEP, with very high ΔNDEP in the past 5 decades (from 1.5 gN m^{-2} yr^{-1} to 5 gN m^{-2} yr^{-1}) (Fig 5c, 5d and S1). eCO_2 also induced significant leaf C:N ratio increase, especially in southwestern China where NDEP was lower (0.3 gN m^{-2} yr^{-1}) (Fig 5b and 5d). Overall in most area in China, Δleaf C:N was determined by the relative strength between iNDEP and eCO_2 (Fig 5d and 5e). These results are consistent with observations in Europe, reporting that tree leaf nitrogen concentration became lower in low nitrogen deposition area in north Europe, and by contrast, in central Europe where nitrogen deposition was higher, leaf nitrogen concentration did not decrease (Jonard et al., 2015; Mellert and Göttlein, 2012).

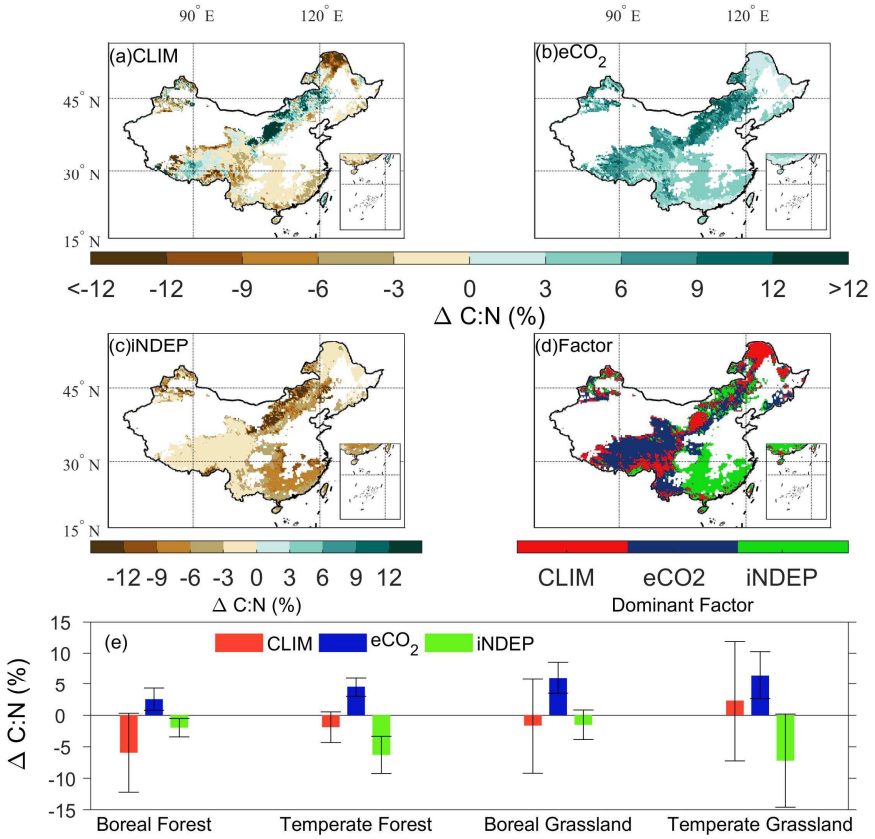

Figure 5. Leaf C:N ratio sensitivities to environment factors by numerical experiments with CLM5.0; (a) climate change; (b) CO_2 enrichment; (c) nitrogen deposition increase; (d) dominant factor in different region; (e) sensitivities from CLM5.0 averaged by PFT.

The differences between spatial and temporal sensitivities also suggest that the climate envelop mechanism (leaf C:N constrained by climate and its change) may be more appropriate for long-term relationship between leaf traits and environment, when plant groups or species are given sufficient time to replace one another along environmental gradients (Yang et al., 2019), but not at the first order to influence the leaf C:N change in decade scale. By contrast, soil N uptake and supply in soil-microbe-plant biogeochemical processes are likely to dominate the leaf C:N change in decade scale. Soil nutrient availability dominating the maintenance of plant stoichiometric homeostasis was widely observed empirically (Luo et al., 2021; Schreeg et al.,

2014; Yan et al., 2014; Yu et al., 2010). In this study, with CLM5.0 nitrogen cycle modelling results, soil N availably under environmental change was deduced to be dominated by iNDEP and warming. iNDEP was found as the most important nitrogen source that changed soil mineral nitrogen supply in China, especially in temperate ecosystems (50% contribution for temperate forest, 70% contribution for temperate grassland Fig 6d and Fig 6e), and was also the dominant factor to soil mineral nitrogen pool change (Fig S14a). In boreal ecosystems, nitrogen release from soil organic matter decomposition (net nitrogen mineralization) was the primary supplier to soil nitrogen, contributing 55% for boreal forest and 80% for boreal grassland (Fig 6e). The importance of atmospheric N deposition to soil mineral N was widely reported (Geng et al., 2021; Marty et al., 2017; Mgelwa et al., 2020), indicating that iNDEP increasing soil N availability could be a dominating mechanism to influence leaf C:N ratio change in China. Besides, our results also confirm previous studies that reported a dilution effect under eCO_2 with a lower leaf N concentration (Deng et al., 2015; Sardans et al., 2017). This probably was related to progressive N limitation, PNL (Luo et al., 2004; Reich et al., 2006), and caused by the unbalance of soil N uptake demand and supply.

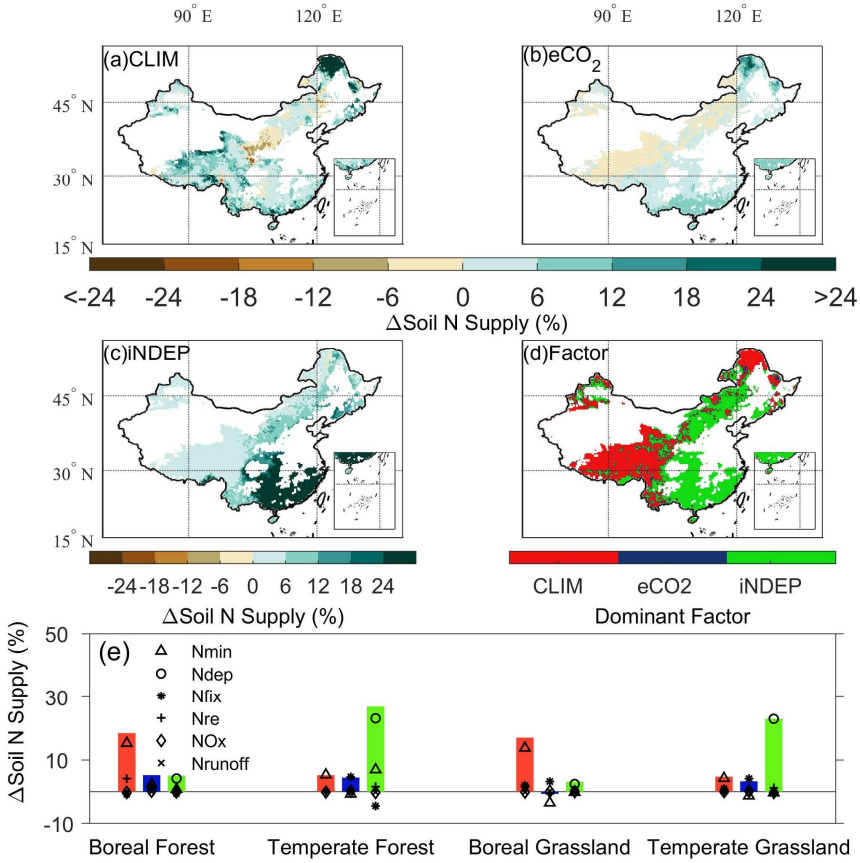

Figure 6. Soil mineral nitrogen supply temporal variation simulated by CLM5.0; (a) climate change; (b) CO_2 enrichment; (c) nitrogen deposition increase; (d) dominant factor; (e) result averaged by PFT. Nmin is for net nitrogen mineralization; Ndep is for nitrogen deposition; Nfix is for biological nitrogen fixation; Nre is for nitrogen translocation, NOx is for NOx (NO and N_2O) emission in denitrification process, Nrunoff is for soil nitrogen leaching loess.

4.2 Implication to carbon cycle modelling

Recently, two major changes are being made to improve carbon cycle models, one is enabling flexible plant trait coupling (Fisher et al., 2015; Peaucelle et al., 2019; Scheiter et al., 2013), the other focuses on incorporating nutrient limitation processes (Shi et al., 2016; Wang et

al., 2010; Zaehle et al., 2014; Zhu et al., 2019). Improving leaf stoichiometry and representing its flexibility is at the intersection of these two changes.

First, we infer that the climate envelope theory of trait-environment interaction is likely not suitable for modeling leaf stoichiometry at decade scale. Therefore, we should be cautious on employing simple trait and environment regression relationships in dynamic vegetation models or land surface models (Verheijen et al., 2015; Walker et al., 2017). By contrast, results from the process-based model CLM5.0 which assumes nutrient acquisition to be balanced with metabolic cost are consistent with relationships inferred from both plot data and data-driven model (Fig 2), indicating the trade-off theory is likely more reasonable.

The FUN model used in CLM5.0 is one of the first to represent the interaction between plant and microbe nutrient uptake interaction (Fisher et al., 2010; Shi et al., 2016), which is a possible scheme to reflect plant trade-off between resources acquisition and conservation. The scheme represented plant-microbial symbiosis explicitly, which was observed in more and more filed studies (Terrer et al., 2016; Terrer et al., 2018). Even though the process representation is very simple and empirical, it likely has improved the model performance by incorporating these complex interactions between plant, microbe and soil.

Second, we corroborate previous studies that flexible plant CN ratio is likely to have a significant impact on modeled carbon cycle (Caldararu et al., 2020; Peaucelle et al., 2019; Walker et al., 2017). V_{cmax25} is observed to be highly correlated to leaf C:N ratio change and presented an opposite direction to leaf C:N ratio change. Here CLM5.0 predicts that V_{cmax25} in northwestern China has decreased about 10%, while in southeastern China has increased about 10% caused by leaf C:N ratio change (Fig 7a). The increase of V_{cmax25} was often higher than N uptake cost (Fig 7b). Therefore, the flexible CN scheme tends to increase plant carbon

509 assimilation for most areas, leading to higher NPP and LAI (Fig 7c and 7d). Further, CLM5.0
510 predicts that grassland ecosystem responded more strongly in NPP and LAI than forest
511 ecosystem (about 16% ± 20% vs 5% ± 8%)(Figure 7e). Hence, given the continuously
512 increasing atmospheric CO_2 concentration and N deposition in the world, the flexible plant
513 stoichiometry scheme is essential in carbon cycle modelling and projection.

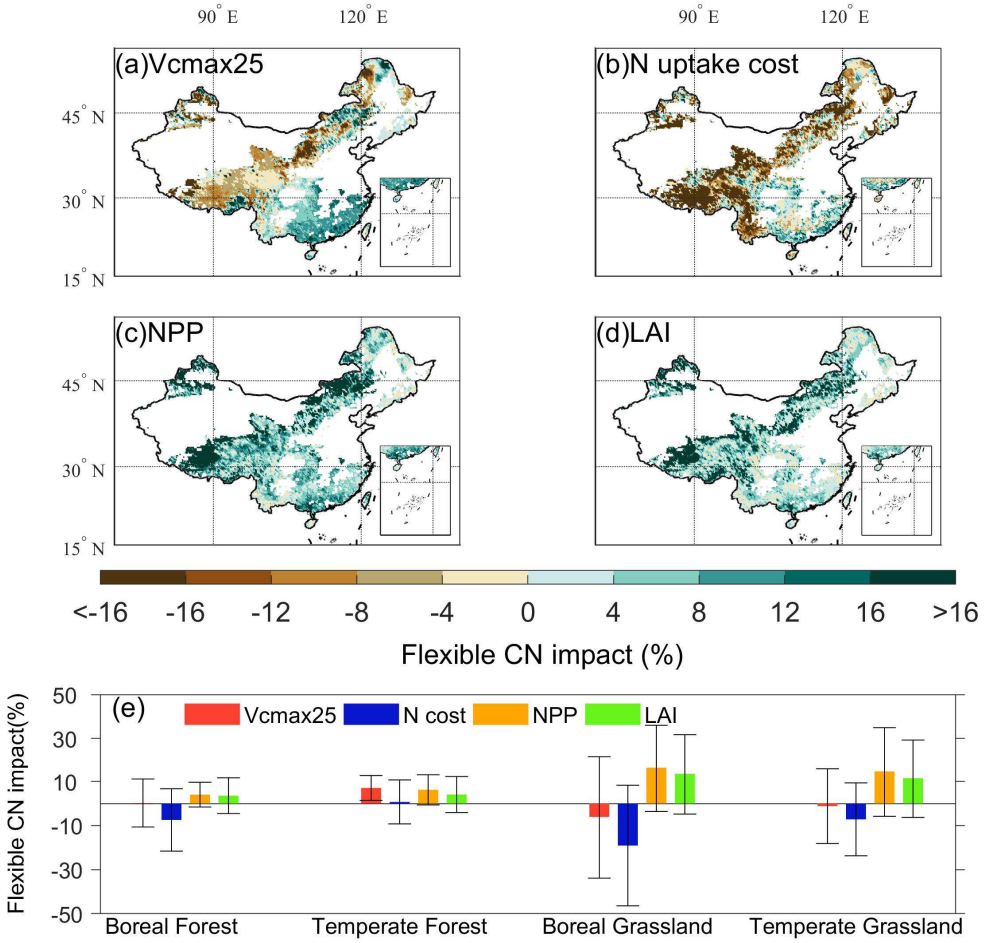

514

515 **Figure 7.** Flexible CN ratio impact on carbon cycle modelling in CLM5.0; (a) V_{cmax25}; (b)
516 nitrogen acquisition cost; (c) net primary productivity (NPP); (d) leaf area index (LAI); (e)
517 results average by PFT.

518 4.3 Limitation and prospection

519 We noticed that the data-driven model and the process-based CLM5.0 were making
520 different predictions. Generally, the leaf C:N ratio sensitivities to both eCO_2 and iNDEP in
521 CLM5.0 are lower than those in the data-driven model. The increasing leaf C:N ratios in low
522 NDEP area predicted by CLM5.0 are around 50% lower than in the data-driven model, and the
523 decreasing leaf C:N ratios in high NDEP area are around 70% lower than in the data-driven
524 model (Fig 2). The experimental manipulations of CLM5.0 also reported these weak LNC
525 sensitivities (Wieder et al., 2019).

526 Here, we reckon two possible reasons for these weak sensitivities. First, the meaning and
527 representativeness of leaf C:N ratios in data-driven model and CLM5.0 are slightly different. The
528 measurement data mainly sampled photosynthetic productive leaves of plant, which are likely to
529 have a stronger LNC variation within canopy. Field measurement reported that the bottom
530 canopy layer had a stronger LNC seasonal variation than upper canopy during the growing
531 season (Coble et al., 2016). Leaf spectroscopy by remote sensing also revealed higher variation
532 in sun-lit leaf LNC (Yang et al., 2016).The vertical LNC pattern within canopy is constrained by
533 hydraulic conductance, bottom canopy leaves tend to have a higher LNC within canopy (Coble
534 et al., 2016; Niinemets, 2012). These observations thus indicated that the higher canopy leaves
535 formed by stimulated carbon assimilation under eCO_2 have a larger chance to decrease LNC due
536 to the coupling between nitrogen and water transport. By contrast, the process-based model
537 CLM5.0 uses a big leaf model and assumes all leaves as one plant organ of the same nutrient
538 variation, and is thus unable to represent the within canopy LNC difference.

539 Second, there could be missing mechanisms in the LNC variation representation in
540 CLM5.0. For example, field measurement revealed that elevated CO_2 could limit nitrogen

transportation from soil to leaf with less transpiration (McDonald et al., 2002; McGrath and Lobell, 2013), by contrast, iNDEP was likely to enhance transpiration (Zhou et al., 2017) to transport more nitrogen to canopy. Therefore, by lacking a linkage between nutrient-mass flow and transpiration, CLM5.0 tends to underestimate the LNC response to eCO_2 and iNDEP. Furthermore, in field manipulation experiments, leaf C:N ratio was found to be most sensitive to both eCO_2 and nitrogen addition, by contrast, woody structure tissues had the lowest sensitivity (Du et al., 2019; Xia and Wan, 2008; Yang et al., 2011). These observations indicate that plant carbon and nitrogen tissue allocation strategies could be very different. For woody plants, root and leaf tend to have less increase in biomass but larger increase in nitrogen concentration in nitrogen addition experiments, by contrast the stem and branch nitrogen concentrations increase at a rate 30% lower, but biomass is three times faster (Wang et al., 2017; Xia and Wan, 2008). Beyond lacking this mechanism, CLM5.0 is also incapable of capturing the different C:N ratio sensitivities across different plant tissues. In contrast to empirical observations, CLM5.0 shows a very similar carbon and nitrogen increasing response across different tissues to both eCO_2 and iNDEP, thus the leaf C:N ratio sensitivity could be underestimate by this relatively fixed C and N allocation strategy (Fig S15, Fig S16).

In order to make the modeling results more consistent with leaf trait observations, we recommend improvements in three aspects: 1) more carbon and nitrogen concentration trait measurements within different canopy layers and across different tissues should be acquired. They will help reveal how different the C:N ratio response to environment change within canopy layers and across tissues, and the mechanism behind them; 2) the process-based LSMs should focus on explicit representation of canopy structure and vertical leaf trait dynamics, and the big leaf model with static canopy scaling parameters was improper compared with observations

(Rogers et al., 2017). Fortunately, there are efforts underway to address this model insufficiency (e.g.,(e.g., Fisher et al., 2018; Koven et al., 2019)). 3) Further studies and quantitative relations should be explored on the linkage between transpiration, hydraulic conductance and plant nitrogen concentration profile, and the mechanism about difference in carbon and nitrogen allocation strategies across plant tissues.

5 Conclusion

In this study, we employed both a data-driven model and a process-based model CLM5.0 to map the leaf C:N ratio spatiotemporal variation in China in the past 5 decades. We found that leaf C:N ratio had a temporally significant but spatially uneven pattern of change. We found an increasing leaf C:N ratio for temperate grassland in northern China (about +5.3% ± 8.2%) and for boreal grassland in western China (about +3.3% ± 6.6%), by contrast a decrease for temperate forest in southern China (about -7.7% ± 6.6%) and for boreal forest in northeastern China (about -3.3% ± 5.5%). In addition, the structural equation models indicated that the temporal leaf C:N change was sensitive to ΔNDEP, ΔCO_2 and ΔMAT rather than to ΔMAP and ecosystem types. These relationship were supported by CLM5.0 scenario analysis, where nitrogen deposition was the dominant factor that led to leaf C:N ratio decreasing in southern China. Elevating CO_2 is likely to increase leaf C:N ratio in low NDEP area. Climate change has stronger impact in boreal area than in temperate area with more net nitrogen mineralization increases in boreal area under climate warming.

Furthermore, the study also found the differences between leaf C:N spatial and temporal variation sensitivities, suggesting that the climate envelope theory was more suitable to predict long-term variation but had limitation to model trait-environment change in leaf C:N ratio at decade scale, and highlight the important role of nitrogen acquisition cost and soil nitrogen

587 availability in determining leaf C:N ratio. Finally, we inferred that there is significant impact of
588 flexible leaf C:N ratio on plant and ecosystem carbon cycling, and it is important for models to
589 incorporate plant and microbial interaction and their carbon cost during plant nitrogen uptake.
590 The leaf C:N ratio response predicted by two models agree with filed observation, but CLM5.0
591 showed weaker magnitude. The poor performance of CLM5.0 is likely due to insufficient
592 representation of within canopy leaf trait dynamics, linkage between transpiration, hydraulic
593 conductance and plant nitrogen concentration profile, and differences in carbon and nitrogen
594 allocation strategies across plant tissues in CLM5.0, all of which should be further explored in
595 future studies.
596

597 **Acknowledgments**

598 In this research, M. Y. Sheng and D.W. Yang are supported by the National Natural Science
599 Foundation of China (Project No. 42041004). J.Y. Tang is supported by the Director, Office of
600 Science, Office of Biological and Environmental Research of the US Department of Energy
601 under contract No. DE-AC02- 05CH11231 as part of RUBISCO project under the Regional and
602 Global Climate Modeling (RGCM) Program. CLM5.0 was acquired from NCAR
603 (www.cesm.ucar.edu/models/clm/).
604
605

606 **References**

607 Ainsworth EA, Long SP. What have we learned from 15 years of free-air CO2 enrichment (FACE)? A meta-analytic
608 review of the responses of photosynthesis, canopy properties and plant production to rising CO2. New
609 Phytol 2005; 165: 351-71.

610 Atkin OK, Bloomfield KJ, Reich PB, Tjoelker MG, Asner GP, Bonal D, et al. Global variability in leaf respiration
611 in relation to climate, plant functional types and leaf traits. New Phytol 2015; 206: 614-36.
612 Bai E, Li S, Xu W, Li W, Dai W, Jiang P. A meta-analysis of experimental warming effects on terrestrial nitrogen
613 pools and dynamics. New Phytol 2013; 199: 441-451.
614 Butler EE, Datta A, Flores-Moreno H, Chen M, Wythers KR, Fazayeli F, et al. Mapping local and global variability
615 in plant trait distributions. Proc Natl Acad Sci U S A 2017; 114: E10937-E10946.
616 Caldararu S, Thum T, Yu L, Zaehle S. Whole-plant optimality predicts changes in leaf nitrogen under variable CO2
617 and nutrient availability. New Phytol 2020; 225: 2331-2346.
618 Coble AP, VanderWall B, Mau A, Cavaleri MA. How vertical patterns in leaf traits shift seasonally and the
619 implications for modeling canopy photosynthesis in a temperate deciduous forest. Tree Physiol 2016; 36:
620 1077-91.
621 Cornelissen JHC, Lavorel S, Garnier E, Diaz S, Buchmann N, Gurvich DE, et al. A handbook of protocols for
622 standardised and easy measurement of plant functional traits worldwide. Australian Journal of Botany
623 2003; 51: 335-380.
624 Crous KY, Reich PB, Hunter MD, Ellsworth DS. Maintenance of leaf N controls the photosynthetic CO2 response
625 of grassland species exposed to 9 years of free-air CO2 enrichment. Global Change Biology 2010; 16:
626 2076-2088.
627 d'Annunzio R, Zeller B, Nicolas M, Dhôte J-F, Saint-André L. Decomposition of European beech (Fagus sylvatica)
628 litter: Combining quality theory and 15N labelling experiments. Soil Biology and Biochemistry 2008; 40:
629 322-333.
630 Deng Q, Hui D, Luo Y, Elser J, Wang Y-P, Loladze I, et al. Down-regulation of tissue N:P ratios in terrestrial plants
631 by elevated CO2. Ecology 2015; 96: 3354-3362.
632 Doughty CE, Goldsmith GR, Raab N, Girardin CAJ, Farfan-Amezquita F, Huaraca-Huasco W, et al. What controls
633 variation in carbon use efficiency among Amazonian tropical forests? Biotropica 2018; 50: 16-25.
634 Du C, Wang X, Zhang M, Jing J, Gao Y. Effects of elevated CO2 on plant C-N-P stoichiometry in terrestrial
635 ecosystems: A meta-analysis. Sci Total Environ 2019; 650: 697-708.
636 Ellsworth DS, Reich PB, Naumburg ES, Koch GW, Kubiske ME, Smith SD. Photosynthesis, carboxylation and leaf
637 nitrogen responses of 16 species to elevated pCO2 across four free-air CO2 enrichment experiments in
638 forest, grassland and desert. Global Change Biology 2004; 10: 2121-2138.
639 Evans JR. Photosynthesis and nitrogen relationships in leaves of C3 plants. Oecologia 1989; 78: 9-19.
640 Evans JR, Poorter H. Photosynthetic acclimation of plants to growth irradiance: the relative importance of specific
641 leaf area and nitrogen partitioning in maximizing carbon gain. Plant Cell and Environment 2001; 24: 755-
642 767.
643 Fisher JB, Sitch S, Malhi Y, Fisher RA, Huntingford C, Tan SY. Carbon cost of plant nitrogen acquisition: A
644 mechanistic, globally applicable model of plant nitrogen uptake, retranslocation, and fixation. Global
645 Biogeochemical Cycles 2010; 24: n/a-n/a.
646 Fisher RA, Koven CD, Anderegg WRL, Christoffersen BO, Dietze MC, Farrior CE, et al. Vegetation demographics
647 in Earth System Models: A review of progress and priorities. Global Change Biology 2018; 24: 35-54.
648 Fisher RA, Muszala S, Verteinstein M, Lawrence P, Xu C, McDowell NG, et al. Taking off the training wheels: the
649 properties of a dynamic vegetation model without climate envelopes, CLM4.5(ED). Geoscientific Model
650 Development 2015; 8: 3593-3619.
651 Geng J, Li H, Chen D, Nei X, Diao Y, Zhang W, et al. Atmospheric nitrogen deposition and its environmental
652 implications at a headwater catchment of Taihu Lake Basin, China. Atmospheric Research 2021; 256.
653 Ghimire B, Riley WJ, Koven CD, Mu MQ, Randerson JT. Representing leaf and root physiological traits in CLM
654 improves global carbon and nitrogen cycling predictions. Journal of Advances in Modeling Earth Systems
655 2016; 8: 598-613.
656 Han W, Fang J, Guo D, Zhang Y. Leaf nitrogen and phosphorus stoichiometry across 753 terrestrial plant species in
657 China. New Phytol 2005; 168: 377-85.
658 Harris I, Jones PD, Osborn TJ, Lister DH. Updated high-resolution grids of monthly climatic observations - the
659 CRU TS3.10 Dataset. International Journal of Climatology 2014; 34: 623-642.
660 Hessen DO, Ågren GI, Anderson TR, Elser JJ, de Ruiter PC. Carbon Sequestration in Ecosystems: The Role of
661 Stoichiometry. Ecology 2004; 85: 1179-1192.
662 Hijmans RJ, Graham CH. The ability of climate envelope models to predict the effect of climate change on species
663 distributions. Global Change Biology 2006; 12: 2272-2281.
664 Hu YK, Liu XY, He NP, Pan X, Long SY, Li W, et al. Global patterns in leaf stoichiometry across coastal wetlands.
665 Global Ecology and Biogeography 2021; 30: 852-869.

Huang W, Houlton BZ, Marklein AR, Liu J, Zhou G. Plant stoichiometric responses to elevated CO2 vary with nitrogen and phosphorus inputs: Evidence from a global-scale meta-analysis. Sci Rep 2015; 5: 18225.
Jonard M, Furst A, Verstraeten A, Thimonier A, Timmermann V, Potocic N, et al. Tree mineral nutrition is deteriorating in Europe. Glob Chang Biol 2015; 21: 418-30.
Kattge J, Diaz S, Lavorel S, Prentice C, Leadley P, Bonisch G, et al. TRY - a global database of plant traits. Global Change Biology 2011; 17: 2905-2935.
Kattge J, Knorr W. Temperature acclimation in a biochemical model of photosynthesis: a reanalysis of data from 36 species. Plant Cell Environ 2007; 30: 1176-90.
Kong D, Ma C, Zhang Q, Li L, Chen X, Zeng H, et al. Leading dimensions in absorptive root trait variation across 96 subtropical forest species. New Phytol 2014; 203: 863-72.
Koven CD, Knox RG, Fisher RA, Chambers J, Christoffersen BO, Davies SJ, et al. Benchmarking and Parameter Sensitivity of Physiological and Vegetation Dynamics using the Functionally Assembled Terrestrial Ecosystem Simulator (FATES) at Barro Colorado Island, Panama. Biogeosciences Discuss. 2019; 2019: 1-46.
Lawrence DM, Fisher RA, Koven CD, Oleson KW, Swenson SC, Bonan G, et al. The Community Land Model Version 5: Description of New Features, Benchmarking, and Impact of Forcing Uncertainty. Journal of Advances in Modeling Earth Systems 2019; 11: 4245-4287.
Lawrence DM, Hurtt GC, Arneth A, Brovkin V, Calvin KV, Jones AD, et al. The Land Use Model Intercomparison Project (LUMIP) contribution to CMIP6: rationale and experimental design. Geoscientific Model Development 2016; 9: 2973-2998.
Lefcheck JS, Freckleton R. piecewiseSEM: Piecewise structural equation modelling in r for ecology, evolution, and systematics. Methods in Ecology and Evolution 2015; 7: 573-579.
Lei H, Yang D, Huang M. Impacts of climate change and vegetation dynamics on runoff in the mountainous region of the Haihe River basin in the past five decades. Journal of Hydrology 2014; 511: 786-799.
Leuzinger S, Luo Y, Beier C, Dieleman W, Vicca S, Korner C. Do global change experiments overestimate impacts on terrestrial ecosystems? Trends Ecol Evol 2011; 26: 236-41.
Li Y, Zhang Y, Zhang X, Korpelainen H, Berninger F, Li C. Effects of elevated CO2 and temperature on photosynthesis and leaf traits of an understory dwarf bamboo in subalpine forest zone, China. Physiol Plant 2013; 148: 261-72.
Liu J, Zhang Z, Xu X, Kuang W, Zhou W, Zhang S, et al. Spatial patterns and driving forces of land use change in China during the early 21st century. Journal of Geographical Sciences 2010; 20: 483-494.
Liu J, Zhou G, Xu Z, Duan H, Li Y, Zhang D. Photosynthesis acclimation, leaf nitrogen concentration, and growth of four tree species over 3 years in response to elevated carbon dioxide and nitrogen treatment in subtropical China. Journal of Soils and Sediments 2011; 11: 1155-1164.
Liu X, Zhang Y, Han W, Tang A, Shen J, Cui Z, et al. Enhanced nitrogen deposition over China. Nature 2013; 494: 459-62.
Lü C, Tian H. Spatial and temporal patterns of nitrogen deposition in China: Synthesis of observational data. Journal of Geophysical Research 2007; 112.
Luo Y, Peng Q, Li K, Gong Y, Liu Y, Han W. Patterns of nitrogen and phosphorus stoichiometry among leaf, stem and root of desert plants and responses to climate and soil factors in Xinjiang, China. Catena 2021; 199.
Luo Y, Su B, Currie WS, Dukes JS, Finzi A, Hartwig U, et al. Progressive nitrogen limitation of ecosystem responses to rising atmospheric carbon dioxide. BioScience 2004; 54: 731-739.
Marty C, Houle D, Gagnon C, Courchesne F. The relationships of soil total nitrogen concentrations, pools and C:N ratios with climate, vegetation types and nitrate deposition in temperate and boreal forests of eastern Canada. Catena 2017; 152: 163-172.
McCarthy HR, Oren R, Finzi AC, Johnsen KH. Canopy leaf area constrains CO2-induced enhancement of productivity and partitioning among aboveground carbon pools. Proc Natl Acad Sci U S A 2006; 103: 19356-61.
McDonald EP, Erickson JE, Kruger EL. Research note: Can decreased transpiration limit plant nitrogen acquisition in elevated CO2? Funct Plant Biol 2002; 29: 1115-1120.
McGrath JM, Lobell DB. Reduction of transpiration and altered nutrient allocation contribute to nutrient decline of crops grown in elevated CO2 concentrations. Plant Cell Environ 2013; 36: 697-705.
McLauchlan KK, Ferguson CJ, Wilson IE, Ocheltree TW, Craine JM. Thirteen decades of foliar isotopes indicate declining nitrogen availability in central North American grasslands. New Phytol 2010; 187: 1135-1145.

720 Mellert KH, Göttlein A. Comparison of new foliar nutrient thresholds derived from van den Burg's literature
721 compilation with established central European references. European Journal of Forest Research 2012; 131:
722 1461-1472.
723 Meyerholt J, Zaehle S. The role of stoichiometric flexibility in modelling forest ecosystem responses to nitrogen
724 fertilization. New Phytol 2015; 208: 1042-55.
725 Mgelwa AS, Kabalika Z, Hu Y-L. Increasing importance of nitrate-nitrogen and organic nitrogen concentrations in
726 bulk and throughfall precipitation across urban forests in southern China. Global Ecology and Conservation
727 2020; 22.
728 Moreno-Martinez A, Camps-Valls G, Kattge J, Robinson N, Reichstein M, van Bodegom P, et al. A methodology to
729 derive global maps of leaf traits using remote sensing and climate data. Remote Sensing of Environment
730 2018; 218: 69-88.
731 Niinemets U. Optimization of foliage photosynthetic capacity in tree canopies: towards identifying missing
732 constraints. Tree Physiol 2012; 32: 505-9.
733 Norby RJ, Sholtis JD, Gunderson CA, Jawdy SS. Leaf dynamics of a deciduous forest canopy: no response to
734 elevated CO2. Oecologia 2003; 136: 574-84.
735 Palmroth S, Oren R, McCarthy HR, Johnsen KH, Finzi AC, Butnor JR, et al. Aboveground sink strength in forests
736 controls the allocation of carbon below ground and its [CO2]-induced enhancement. Proc Natl Acad Sci U
737 S A 2006; 103: 19362-7.
738 Peaucelle M, Bacour C, Ciais P, Vuichard N, Kuppel S, Penuelas J, et al. Covariations between plant functional
739 traits emerge from constraining parameterization of a terrestrial biosphere model. Global Ecology and
740 Biogeography 2019; 28: 1351-1365.
741 Pedregosa F, Varoquaux G, Gramfort A, Michel V, Thirion B, Grisel O, et al. Scikit-learn: Machine Learning in
742 Python. Journal of Machine Learning Research 2011; 12: 2825-2830.
743 Piao S, Ciais P, Huang Y, Shen Z, Peng S, Li J, et al. The impacts of climate change on water resources and
744 agriculture in China. Nature 2010; 467: 43-51.
745 Reich PB. Key canopy traits drive forest productivity. Proc Biol Sci 2012; 279: 2128-34.
746 Reich PB. The world-wide 'fast–slow'plant economics spectrum: a traits manifesto. Journal of Ecology 2014; 102:
747 275-301.
748 Reich PB, Hobbie SE, Lee T, Ellsworth DS, West JB, Tilman D, et al. Nitrogen limitation constrains sustainability
749 of ecosystem response to CO2. Nature 2006; 440: 922-925.
750 Reich PB, Oleksyn J. Global patterns of plant leaf N and P in relation to temperature and latitude. Proceedings of the
751 National Academy of Sciences of the United States of America 2004; 101: 11001.
752 Rogers A, Medlyn BE, Dukes JS, Bonan G, von Caemmerer S, Dietze MC, et al. A roadmap for improving the
753 representation of photosynthesis in Earth system models. New Phytol 2017; 213: 22-42.
754 Running S. MQ, Zhao M. MOD17A2H MODIS/Terra Gross Primary Productivity 8-Day L4 Global 500m SIN Grid
755 V006. In: DAAC NELP, editor, 2015.
756 Sardans J, Grau O, Chen HYH, Janssens IA, Ciais P, Piao S, et al. Changes in nutrient concentrations of leaves and
757 roots in response to global change factors. Glob Chang Biol 2017; 23: 3849-3856.
758 Sardans J, Rivas-Ubach A, Peñuelas J. The C:N:P stoichiometry of organisms and ecosystems in a changing world:
759 A review and perspectives. Perspectives in Plant Ecology, Evolution and Systematics 2012; 14: 33-47.
760 Scheiter S, Langan L, Higgins SI. Next-generation dynamic global vegetation models: learning from community
761 ecology. New Phytol 2013; 198: 957-969.
762 Schreeg LA, Santiago LS, Wright SJ, Turner BL. Stem, root, and older leaf N:P ratios are more responsive
763 indicators of soil nutrient availability than new foliage. Ecology 2014; 95: 2062-2068.
764 Shangguan W, Dai YJ, Liu BY, Ye AZ, Yuan H. A soil particle-size distribution dataset for regional land and
765 climate modelling in China. Geoderma 2012; 171: 85-91.
766 Shi M, Fisher JB, Brzostek ER, Phillips RP. Carbon cost of plant nitrogen acquisition: global carbon cycle impact
767 from an improved plant nitrogen cycle in the Community Land Model. Glob Chang Biol 2016; 22: 1299-
768 314.
769 Sigurdsson BD, Medhurst JL, Wallin G, Eggertsson O, Linder S. Growth of mature boreal Norway spruce was not
770 affected by elevated CO2 and/or air temperature unless nutrient availability was improved. Tree Physiol
771 2013; 33: 1192-205.
772 Song W, Deng X. Land-use/land-cover change and ecosystem service provision in China. Sci Total Environ 2017;
773 576: 705-719.

774 Soudzilovskaia NA, Elumeeva TG, Onipchenko VG, Shidakov II, Salpagarova FS, Khubiev AB, et al. Functional
775 traits predict relationship between plant abundance dynamic and long-term climate warming. Proceedings
776 of the National Academy of Sciences of the United States of America 2013; 110: 18180-18184.
777 Sterner RW, Elser JJ. Ecological Stoichiometry: The Biology of Elements from Molecules to the Biosphere:
778 Princeton University Press, 2002.
779 Tang Z, Xu W, Zhou G, Bai Y, Li J, Tang X, et al. Patterns of plant carbon, nitrogen, and phosphorus concentration
780 in relation to productivity in China's terrestrial ecosystems. Proceedings of the National Academy of
781 Sciences 2018; 115: 4033.
782 Terrer C, Vicca S, Hungate BA, Phillips RP, Prentice IC. Mycorrhizal association as a primary control of the CO2
783 fertilization effect. Science 2016; 353: 72-4.
784 Terrer C, Vicca S, Stocker BD, Hungate BA, Phillips RP, Reich PB, et al. Ecosystem responses to elevated CO2
785 governed by plant-soil interactions and the cost of nitrogen acquisition. New Phytol 2018; 217: 507-522.
786 Verheijen LM, Aerts R, Brovkin V, Cavender-Bares J, Cornelissen JH, Kattge J, et al. Inclusion of ecologically
787 based trait variation in plant functional types reduces the projected land carbon sink in an earth system
788 model. Glob Chang Biol 2015; 21: 3074-86.
789 Vitousek PM, Turner DR, Kitayama K. Foliar Nutrients During Long-Term Soil Development in Hawaiian Montane
790 Rain Forest. Ecology 1995; 76: 712-720.
791 Walker AP, Quaife T, van Bodegom PM, De Kauwe MG, Keenan TF, Joiner J, et al. The impact of alternative trait-
792 scaling hypotheses for the maximum photosynthetic carboxylation rate (Vcmax) on global gross primary
793 production. New Phytol 2017; 215: 1370-1386.
794 Wang D, He HL, Gao Q, Zhao CZ, Zhao WQ, Yin CY, et al. Effects of short-term N addition on plant biomass
795 allocation and C and N pools of theSibiraea angustatascrub ecosystem. European Journal of Soil Science
796 2017; 68: 212-220.
797 Wang YP, Law RM, Pak B. A global model of carbon, nitrogen and phosphorus cycles for the terrestrial biosphere.
798 Biogeosciences 2010; 7: 2261-2282.
799 Weih M, Karlsson PS. Growth response of Mountain birch to air and soil temperature: is increasing leaf-nitrogen
800 content an acclimation to lower air temperature? New Phytologist 2001; 150: 147-155.
801 Wieder WR, Lawrence DM, Fisher RA, Bonan GB, Cheng SJ, Goodale CL, et al. Beyond Static Benchmarking:
802 Using Experimental Manipulations to Evaluate Land Model Assumptions. Global Biogeochem Cycles
803 2019; 33: 1289-1309.
804 Woods HA, Makino W, Cotner JB, Hobbie SE, Harrison JF, Acharya K, et al. Temperature and the chemical
805 composition of poikilothermic organisms. Functional Ecology 2003; 17: 237-245.
806 Wright IJ, Reich PB, Cornelissen JHC, Falster DS, Groom PK, Hikosaka K, et al. Modulation of leaf economic traits
807 and trait relationships by climate. Global Ecology and Biogeography 2005; 14: 411-421.
808 Xia J, Wan S. Global response patterns of terrestrial plant species to nitrogen addition. New Phytol 2008; 179: 428-
809 439.
810 Yan Z, Kim N, Han W, Guo Y, Han T, Du E, et al. Effects of nitrogen and phosphorus supply on growth rate, leaf
811 stoichiometry, and nutrient resorption of Arabidopsis thaliana. Plant and Soil 2014; 388: 147-155.
812 Yang X, Tang JW, Mustard JF, Wu J, Zhao KG, Serbin S, et al. Seasonal variability of multiple leaf traits captured
813 by leaf spectroscopy at two temperate deciduous forests. Remote Sensing of Environment 2016; 179: 1-12.
814 Yang Y, Wang H, Harrison SP, Prentice IC, Wright IJ, Peng C, et al. Quantifying leaf-trait covariation and its
815 controls across climates and biomes. New Phytol 2019; 221: 155-168.
816 Yang YH, Luo YQ, Lu M, Schadel C, Han WX. Terrestrial C:N stoichiometry in response to elevated CO2 and N
817 addition: a synthesis of two meta-analyses. Plant and Soil 2011; 343: 393-400.
818 Yu G, Jia Y, He N, Zhu J, Chen Z, Wang Q, et al. Stabilization of atmospheric nitrogen deposition in China over the
819 past decade. Nature Geoscience 2019; 12: 424-429.
820 Yu Q, Chen Q, Elser JJ, He N, Wu H, Zhang G, et al. Linking stoichiometric homoeostasis with ecosystem
821 structure, functioning and stability. Ecol Lett 2010; 13: 1390-9.
822 Yuan ZY, Chen HYH. Global-scale patterns of nutrient resorption associated with latitude, temperature and
823 precipitation. Global Ecology and Biogeography 2009; 18: 11-18.
824 Yue K, Fornara DA, Yang W, Peng Y, Li Z, Wu F, et al. Effects of three global change drivers on terrestrial C:N:P
825 stoichiometry: a global synthesis. Glob Chang Biol 2017; 23: 2450-2463.
826 Zaehle S, Medlyn BE, De Kauwe MG, Walker AP, Dietze MC, Hickler T, et al. Evaluation of 11 terrestrial carbon–
827 nitrogen cycle models against observations from two temperate Free-Air CO2 Enrichment studies. New
828 Phytologist 2014; 202: 803-822.

Zhou S, Yu BF, Schwalm CR, Ciais P, Zhang Y, Fisher JB, et al. Response of Water Use Efficiency to Global Environmental Change Based on Output From Terrestrial Biosphere Models. Global Biogeochemical Cycles 2017; 31: 1639-1655.

Zhu J, He N, Wang Q, Yuan G, Wen D, Yu G, et al. The composition, spatial patterns, and influencing factors of atmospheric wet nitrogen deposition in Chinese terrestrial ecosystems. Sci Total Environ 2015; 511: 777-85.

Zhu Q, Riley WJ, Tang JY, Collier N, Hoffman FM, Yang XJ, et al. Representing Nitrogen, Phosphorus, and Carbon Interactions in the E3SM Land Model: Development and Global Benchmarking. Journal of Advances in Modeling Earth Systems 2019; 11: 2238-2258.

Zhu Z, Bi J, Pan Y, Ganguly S, Anav A, Xu L, et al. Global Data Sets of Vegetation Leaf Area Index (LAI)3g and Fraction of Photosynthetically Active Radiation (FPAR)3g Derived from Global Inventory Modeling and Mapping Studies (GIMMS) Normalized Difference Vegetation Index (NDVI3g) for the Period 1981 to 2011. Remote Sensing 2013; 5: 927-948.

1

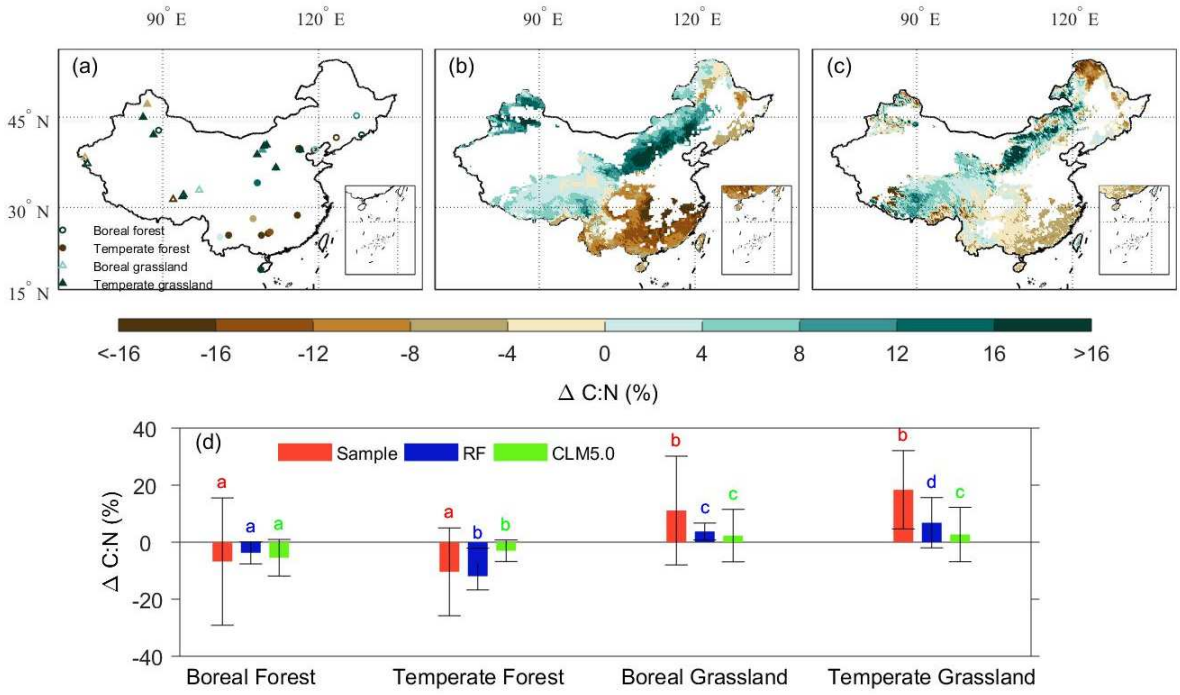

2

3 **Figure.** Temporal variation of multi-annual mean leaf C:N ratio in China (the difference between
4 2 time period from 1960-1989 to 1990-2015); (a) result by plot samples, (b) result by random
5 forest (RF) model, (c) result by CLM5.0; (d) results from all above 3 approaches averaged by
6 PFT. Different lowercase letters in the same color on error bars indicate significant differences
7 across different PFTs at $p < 0.05$.